Analysis of Parallel Drains for Highway Cut-Slope Stabilization

Rodney W. Prellwitz, Forest Service, U.S. Department of Agriculture, Missoula, Montana

Methods of analyzing parallel drains for highway cut-slope stabilization are introduced. The analysis procedure is based on the prediction of the phreatic surface location within a soil mass under steady-state seepage. Relative effectiveness of alternate drain spacings is determined by estimating the steady-state phreatic surface at a profile located midway between drains and by using analysis procedures for the design of parallel drains in agricultural field drainage. Applications are made to seepage from an infinite-slope source. Mathematical analyses for estimating steady-state phreatic surfaces at a blanket drain and cut-slope intercept with an infinite-slope seepage source are also introduced. An illustrative design problem is worked out in detail.

Since their introduction by the California Highway Department in 1939, drilled-in parallel drains have proved to be an effective means of achieving highway cut-slope stabilization (1). Unfortunately, little has been written on the analysis of the use of parallel-drain spacing for this purpose. In practice, drain spacings ranging from 3 to 15 m (10 to 50 ft) are often selected on the basis either of experience (1) or of the carrying capacity of the drainpipe (2). A design criterion is needed by which a designer can evaluate, before installation, the effectiveness of alternate parallel-drain spacings in lowering the groundwater, or phreatic, surface at a profile located midway between the drains. A relative stability analysis can then be made to evaluate drainage alternatives.

A recent article by Kenney, Pazin, and Choi (3) introduced a design criterion for evaluating the relative effectiveness of horizontal parallel drains based on predicting the increase in stability (factor of safety) without analyzing phreatic surface drawdown directly. Their solution was compared with that introduced in this paper in an earlier uncondensed draft (4).

BASIS FOR PARALLEL-DRAIN ANALYSIS

Drainage analysis in this paper is based on the following:

1. A predetermined maximum infinite-slope phreatic surface developed under seepage parallel to a drainage barrier in an unconfined aquifer (phreatic surface I in Figures 1 and 2)—seepage is assumed to be steady state at this critical condition;
2. An undrained steady-state phreatic surface extending from phreatic surface I to the intercept with the cut slope (phreatic surface U in Figures 1 and 2);
3. An estimated steady-state phreatic surface for a blanket drain installed at the same attitude as the parallel drains (phreatic surface D in Figures 1 and 2), extending from phreatic surface I to the drain; and
4. A steady-state phreatic surface estimated to exist at a profile midway between and parallel to two adjacent parallel drains (phreatic surface M in Figures 3 and 4). The rationale used is that, if drains are spaced infinitely far apart, phreatic surface M equals phreatic surface U; if spaced infinitely close together, phreatic surface M equals phreatic surface D.

FLOW-NET ANALYSES: PHREATIC SURFACES I, U, AND D

Flow-net solutions are possible for estimating phreatic surfaces U and D by using equipotential drops (Δh) from the infinite-slope phreatic surface I:

$$\Delta h = h \sin\theta \cos\theta \quad (1)$$

where h equals depth from phreatic surface to the drainage barrier and θ equals slope of the drainage barrier. Figure 1 shows the results of the flow-net analyses for phreatic surfaces U and D. Flow-net analyses are time consuming, and mathematical solutions that can be used to approximate these phreatic surfaces would be faster and readily adaptable to computer analyses.

MATHEMATICAL ANALYSES: PHREATIC SURFACES U AND D

Mathematical solutions for phreatic surfaces U and D are not readily found in the literature for infinite-slope seepage conditions. I have modified solutions by Casagrande and Kozeny (5, 6) developed for a reservoir seepage source to approximate phreatic surfaces U and D from an infinite-slope source. One can expect good correlation for phreatic surface U with the results of flow-net analyses for cut slopes with horizontal-to-vertical ratios of 1:1 (45°) or flatter. For cut slopes steeper than 45°, one may use a graphical approximation based on Casagrande's modified basic parabola (5, 6) procedure in conjunction with the following Equation 10 plotted with the origin at the toe of the cut slope.

Applications of mathematical solutions for phreatic surfaces U and D for seepage emanating from a reservoir source, as they apply to the procedure presented in this paper, were made in an earlier draft (4).

Phreatic Surface U

The vertical distance from the toe to the phreatic surface intercept of the cut slope from flow-net analysis (Figure 1) is

$$\Delta h_W = h_W \sin\theta \cos\theta \quad (2)$$

where h_W is the vertical distance from the toe to the projection of phreatic surface I. If the cut slope intercepts the drainage barrier, $h_W = h$. Corrected for approximate mathematical analysis,

$$\text{Set } X_U = 0 \text{ at } Y_{UO} = h_W \sin\theta \cos\theta\,(1 + \tan^2\theta)(1 + \tan^2\beta) \quad (3)$$

where β is the cut slope. For positive values of X_U (toward the toe)

$$Y_U = X_U \tan\beta \quad (4)$$

At the toe, $Y_U = 0$ and $X_{UO} = Y_{UO}/\tan\beta$. For negative values of X_U (toward phreatic surface I)

$$Y_U = (aX_U^2 - 2Y_{UO}X_U + Y_{UO}^2)^{1/2} \quad (5)$$

where a equals $\tan^2\theta$. At the intercept with phreatic surface I

$$Y_{UI} = h_i - X_{UI} \tan\theta \quad (6)$$

and

$$X_{UI} = (h_i^2 - Y_{UO}^2)/(2h_i \tan\theta - 2Y_{UO}) \quad (7)$$

where $h_I = h_W + X_{UO} \tan\theta$.

Phreatic Surface D

At the intercept of the drain with the barrier set $X_D = 0$ and

$$Y_{DO} = h \sin\theta \cos\theta \ (1 + \tan^2\theta) \quad (8)$$

Phreatic surface enters the drain vertically at (positive value for X_D)

$$X_{DO} = \tfrac{1}{2} h \sin\theta \cos\theta \quad (9)$$

For negative values of X_D (toward phreatic surface I)

$$Y_D = (aX_D^2 - bY_{DO} X_D + Y_{DO}^2)^{1/2} \quad (10)$$

where $a = \tan^2\theta$ and $b = Y_{DO}/X_{DO} + aX_{DO}/Y_{DO}$. At the intercept with phreatic surface I

$$Y_{DI} = h - X_{DI} \tan\theta \quad (11)$$

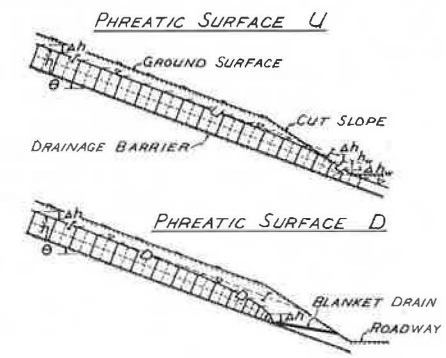

Figure 1. Flow-net analyses for phreatic surfaces U and D.

and

$$X_{DI} = (h^2 - Y_{DO}^2)/(2h \tan\theta - bY_{DO}) \quad (12)$$

If the drain does not intercept the barrier, a solution is possible by setting $X_D = 0$ at the end of the drain and using $h = h_W$ as previously defined.

PARALLEL DRAINS FOR AGRICULTURAL DRAINAGE

Parallel drains have been used successfully in agricultural drainage to lower the phreatic surface to predetermined levels (7, 8). Design criteria exist for both steady-state and transient-state infiltration of rainfall or irrigation water concentrated by a drainage barrier (see Figure 5). The analysis is two-dimensional, and vertical recharge is assumed.

Steady-State Analysis

Where rainfall is frequent, a steady-state analysis is made for the drain spacing (S) required to maintain the phreatic surface at the appropriate level. Figure 5 shows an idealized cross section across two parallel drains under steady-state drainage. The Dutch have pioneered the analysis for the steady-state case, and several solutions are possible (8). The most useful for adaptation to cut-slope stabilization is the Hooghoudt equation:

$$V = (8K_b d h_m + 4K_a h_m^2)/S^2 \quad (13)$$

where

- K_a = hydraulic conductivity (permeability) of the soil above the drainpipe,
- K_b = hydraulic conductivity (permeability) of the soil below the drainpipe,
- V = drain discharge velocity (or rainfall recharge rate),
- h_m = maximum phreatic surface height above the drain

Figure 2. Mathematical analyses for phreatic surfaces U and D.

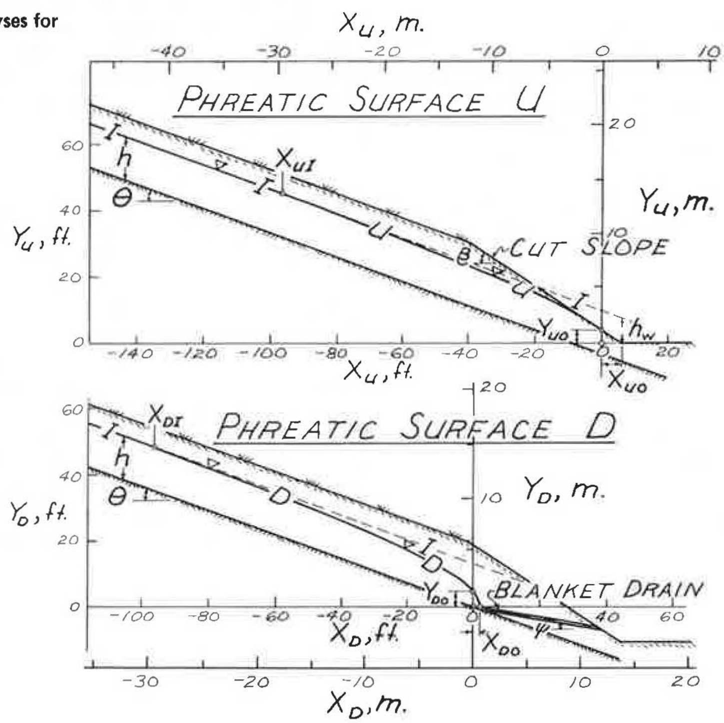

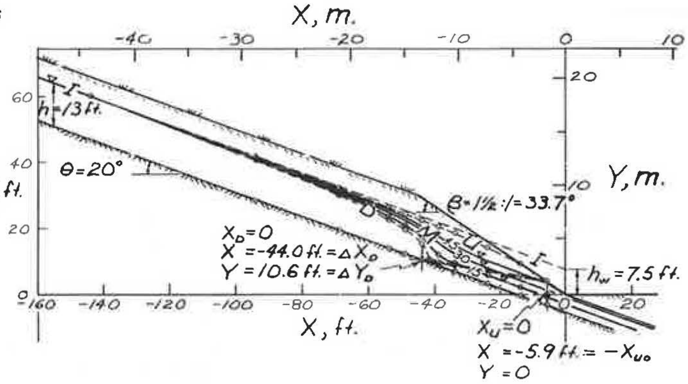

Figure 3. Results of analyses for phreatic surfaces M using three drain spacings.

at a profile midway between the drains,

S = drain spacing,

D = depth from the drain to the drainage barrier, and

d = reduced equivalent depth corresponding to D (reduced to account for extra resistance at the drainpipe caused by radial flow).

For the case where $D < 1/4S$, the relationship between d and D has been developed based on work by Ernst and Hooghoudt (8).

$$d = D/[1 + (8D/\pi S)\ \ln(D/\pi r_o)] \tag{14}$$

where r_o is the radius of the drainpipe.

The typical drilled-in drainpipe used in cut-slope stabilization is slotted PVC plastic with an inside diameter of 3.8 cm (1.5 in). Figure 6 shows the relationship, by Equation 14, between d and D for this drainpipe at various drain spacings.

If the soil is assumed to be homogeneous, then $K_a = K_b = K$, and Equation 13 can be rewritten as an equation for drain spacing:

$$S = \{[4\,K\,h_m\ (2d + h_m)]/V\}^{1/2} \tag{15}$$

Transient-State Analysis

In the case of intermittent recharge, such as with irrigations or high-intensity rainfall, transient- or non-steady-state analysis is used. Figure 5 shows an idealized cross section across two parallel drains under transient-state drainage. The solution for drain spacing (S) is based on lowering the phreatic surface developed by one irrigation (h_o) to a required level (h_t) within the time span (drain-out time) (t) between irrigations so that the following irrigation will not increase the phreatic surface beyond h_o. Several methods of solution are available; the most useful for adaptation to cut-slope drainage is the modified Glover-Dumm equation (8) for the drawdown ratio in the form

$$h_t/h_o = 1.16e^{-\alpha t} \tag{16}$$

where $\alpha t = [\pi^2 K (d + \frac{1}{2}\sqrt{h_o h_t})\ t]/N_e S^2 > 0.2$, N_e is effective porosity (specific yield) of the soil, and K and d are as defined for Equations 13 and 15.

PARALLEL DRAINS FOR HIGHWAY CUT-SLOPE DRAINAGE

The conditions are somewhat different for highway cut-slope drainage than they are for agricultural drainage. Long-term highway cut-slope drainage by parallel drains must be based on (a) steady-state seepage analysis of the maximum groundwater conditions expected during the design life of the highway, (b) recharge at the drains primarily from seepage flow along the drainage barrier, and (c) a three-dimensional analysis.

Figure 7 illustrates the three-dimensional nature of a typical parallel-drain installation for highway cut-slope stabilization. For cross section B-B_1 or C-C_1, as long as seepage is steady, the midpoint phreatic surface heights h_t and h_o, respectively, will not vary with time the way agricultural parallel drains do in the transient state. However, the midpoint phreatic surface height does decrease with successive down-slope cross sections ($h_t < h_o$). This suggests that the two-dimensional transient-state analysis (Equation 16) may be altered to a three-dimensional steady-state analysis (see Figures 5 and 7) by assuming that drains are installed parallel to the gradient of the drainage barrier and defining drain-out time (t) as the time required for seepage to travel between successive down-slope cross sections (C-C_1 to B-B_1).

In addition, the steady-state analysis (Equation 15) may be applicable to the conditions at the end of the drain (cross section C-C_1) if the discharge velocity (V) is defined as a comparable recharge velocity moving along the drainage barrier.

Alteration of the modified Glover-Dumm equation for the three-dimensional steady state can be done as follows. A replacement for drain-out time (t) to represent the time required for seepage to travel between successive down-slope cross sections can be derived by using Darcy's law (1). A variety of solutions is possible depending on the following:

1. How the hydraulic gradient i, equal to ratio between slope distance and slope height, is defined;
2. Whether this hydraulic gradient is assumed constant for a specific vertical cross section; and
3. How the flow distance (Z) between successive cross sections is determined.

Figure 4 illustrates a typical flow situation that might exist on a profile that is midway between drains (M). The most representative hydraulic gradient (i) between successive cross sections is somewhere between the phreatic surface gradient ($\Delta h_P/P$) and the barrier gradient ($\Delta h_B/B$). Also, the most representative flow distance (Z) is somewhere between P and B. The mean values of flow distance and hydraulic gradient are defined, respectively, as

$$Z = (P + B)/2 \tag{17}$$

and

$$i = (\Delta h_P + \Delta h_B)/(P + B) \tag{18}$$

From Darcy's law (1) we can derive an expression for drain-out time (t)

$$Q = K\,i\,A \tag{19}$$

where Q is seepage quantity, A is cross-sectional area normal to the flow, and K and i are as previously defined. Also discharge velocity is

$$V = Q/A = Ki \tag{20}$$

and seepage velocity is

$$V_s = V/N_e = Ki/N_e = Z/t \tag{21}$$

where N_e, Z, and t are as previously defined.
In terms of drain-out time (t),

$$t = Z/V_s = N_e\,Z/Ki \tag{22}$$

Substituting Equation 22 into Equation 16 yields the drawdown ratio

$$h_t/h_o = 1.16e^{-\alpha t} \tag{23}$$

where

$$\alpha t = [\pi^2 (d + ½\sqrt{h_o h_t})\,Z]/S^2 \quad i > 0.2 \tag{24}$$

Alteration of the Hooghoudt equation for the three-dimensional case by substituting V = ki into Equation 15 yields

$$S = \{[4\,h_m(2d + h_m)]/i\}^{½} \tag{25}$$

When the drain contacts the drainage barrier, d = 0, and

$$S = (4\,h_m^{\,2}/i)^{½} \tag{26}$$

Equations 25 and 26 can be used in conjunction with phreatic surfaces U and D to estimate the practical range of drain spacings to be considered in the analysis. The hydraulic gradient is defined in the same manner as in the derivation of Equation 18. For the case where the drain contacts the barrier, the minimum practical drain spacing is

$$S_{min} \cong \{4\,Y_{DO}^{\,2}/\sin[(45° + \theta)/2]\}^{½} \tag{27}$$

where Y_{DO} is from Equation 8, and the maximum practical drain spacing is

$$S_{max} \cong \{4\,h_u^{\,2}/\sin[(\theta_u + \theta)/2]\}^{½} \tag{28}$$

where h_u and θ_u are height above the drain at the barrier and slope at that point, respectively, of phreatic surface U.

ILLUSTRATIVE PROBLEM

To illustrate how the above analysis might be used in an actual design problem, consider the highway cut illustrated in Figures 1 and 2.

Recommended Procedure

A more complete procedure that incorporates this method directly into a slope-stability analysis was given in an earlier draft (4). The following procedure pertains to drainage analysis only.

1. Construct phreatic surface U using either flow-net analysis or mathematical analysis or both (Equations 1-7).
2. Construct phreatic surface D using either flow-net analysis or mathematical analysis or both (Equations 1 and 8-12).
3. Estimate S_{min} and S_{max} using Equations 25-28 and select trial drain spacings.
4. Construct the phreatic surface M for the trial drain spacings. All should fall between phreatic surfaces U and D.
5. Begin the analysis at the intercept of phreatic surfaces D and I from flow-net analysis or Equations 11 and 12.

Figure 4. Definition of hydraulic gradient, drainage distance, and drawdown ratio between successive cross sections.

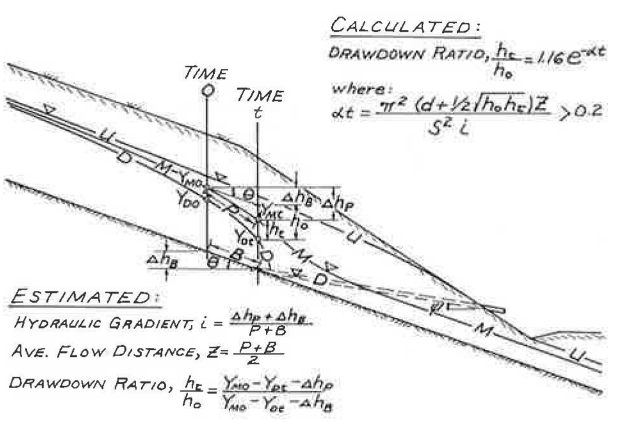

Figure 5. Two-dimensional agricultural drainage with vertical recharge.

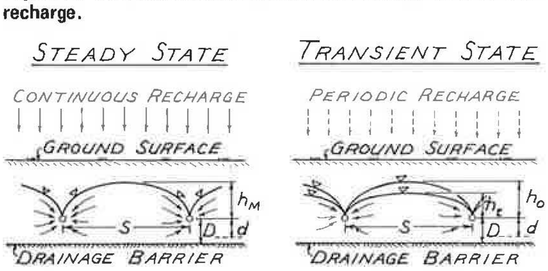

Figure 6. D versus d for a drainpipe of 3.8-cm (1.5-in) inside diameter.

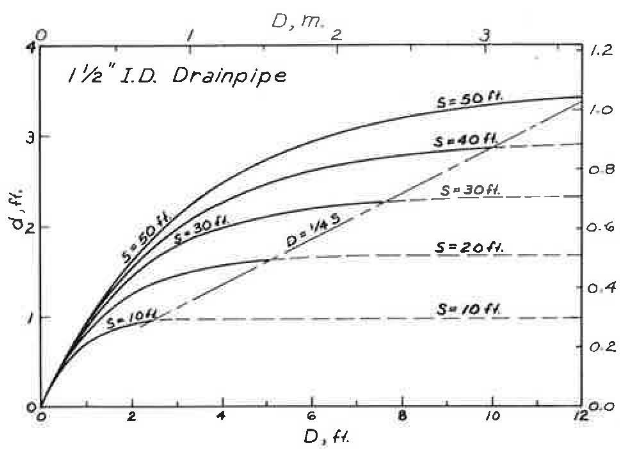

6. Divide into cross sections from intercept D-I(X_{DI}) to the intercept of phreatic surface U with the cut slope (X_{UO}). Cross sections should be spaced far enough apart so that $\alpha t > 0.2$ in Equation 24. Usually spacing larger than S/10 will satisfy this requirement.

7. For negative values of X_D, analyze as if the drain and drainage barrier were both located on phreatic surface D.

8. Between successive cross sections, determine drawdown ratio, h_t/h_o, through trial-and-error relaxation between estimation (see Figure 4) and calculation (Equation 23). Two or three trials are usually sufficient.

<u>Solution</u>

Infinite-slope conditions are h equals 4.0 m (13 ft) and $\theta = 20°$. Refer to Figures 7 and 8 and construct all phreatic surfaces from the same X-Y axis located at the toe of the cut.

Step 1. Phreatic Surface U

From columns 5 and 6 of Figure 8, calculate Equation 3 at $X_U = 0$:

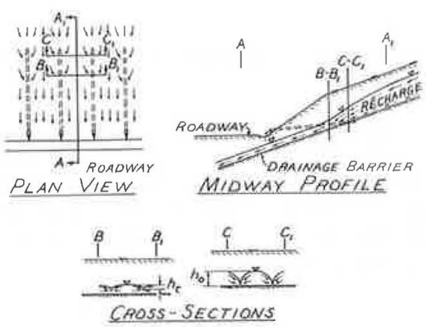

Figure 7. Three-dimensional highway cut-slope drainage with recharge along a drainage barrier.

$Y_{UO} = h_W \sin\theta \cos\theta (1 + \tan^2\theta)(1 + \tan^2\beta) = 1.2$ m (3.9 ft)
Then, with Equation 4 at the toe, $Y_U = 0$ and $X_{UO} = Y_{UO} / \tan\beta = 1.8$ m (5.9 ft)
From Equation 5 for negative values of X_U, we get
$Y_U = (\tan^2\theta X_U^2 - 2\, Y_{UO} X_U + Y_{UO}^2)^{1/2}$ and
$Y_U = (0.132 X_U^2 - 2.40\, X_U + 1.44)^{1/2}$
Plot at
$X = X_U - X_{UO} = X_U - 1.8$
Intercept with phreatic surface I by Equation 7 for
$h_1 = h_W + X_{UO} \tan\theta = 2.9$ m (9.7 ft)
so that
$X_{UI} = (h_1^2 - Y_{UO}^2)/(2h_1 \tan\theta - 2Y_{UO}) = -27.5$ m (-90.3 ft)
at
$X = X_{UI} - X_{UO} = -29.4$ m (-96.2 ft)

Step 2. Phreatic Surface D

From columns 9 and 10 of Figure 8, one can use Equation 8 at the contact of the drain with the barrier; $X_D = 0$ and
$Y_{DO} = h \sin\theta \cos\theta (1 + \tan^2\theta) = 1.4$ m (4.7 ft)
Equation 9 for phreatic surface intercept with drain is
$X_{DO} = \frac{1}{2} h \sin\theta \cos\theta = 0.6$ m (2.1 ft)
Equation 10 for negative values of X_D, where
$a = \tan^2\theta = 0.132$, gives
$b = Y_{DO}/X_{DO} + aX_{DO}/Y_{DO} = 2.32$
where
ΔY_D = conversion to common axis (see Figure 7) = 3.2 m (10.6 ft),
$Y_D = (aX_D^2 - bY_{DO}X_D + Y_{DO}^2)^{1/2} + \Delta Y_D$, and
$Y_D = (0.132X_D^2 - 3.35X_D + 2.08)^{1/2} + 3.2$.
Then plot at $X = X_D + \Delta X_D$, where ΔX_D is the conversion to common axis (see Figure 7)or -13.4 m (-44.0 ft)
$X = X_D - 13.4$
Equation 12 for intercept with phreatic surface I gives
$X_{DI} = (h^2 - Y_{DO}^2)/(2h \tan\theta - bY_{DO}) = -29.2$ m (-95.8 ft)
Begin drain-spacing analysis at $X_D = -30.5$ m (-100 ft) and at $X = X_D - 13.4 = -43.9$ m (-144 ft).

Figure 8. Analysis for phreatic surface M in the problem in Figure 3 with a 4.6-m (15-ft) drain spacing.

PARALLEL DRAIN ANALYSIS - PHREATIC SURFACE CALCULATIONS   Assumed Spacing, S = (1) 15 ft.   Barrier Slope, θ = (2) 20.0 degrees

(3) X	(4) ΔX	U (5) X_U	U (6) Y_U	U (7) ΔY_U	U (8) θ_U	D (9) X_D	D (10) Y_D	M (11) Y_{Mo}	(12) Y_{Mt}	Assumed h_t/h_o (13) Δh_P	(14) Δh_B	(15) $\Delta h_P + \Delta h_B$	(16) θ_M	(17) P	(18) B	(19) P+B	(20) Z	(21) i	(22) $Y_{Mo} - Y_{Dt}$	(23) h_o	(24) h_t	(25) h_t/h_o	Calculated h_t/h_o, + X_D Only: (26) Y_o	(27) D	(28) d	(29) $\frac{\sqrt{h_o h_t}}{2}$	(30) $\alpha t = \frac{\pi^2 (d + \frac{\sqrt{h_o h_t}}{2}) Z}{S^2 i} > 0.2$	(31) h_t/h_o
		(3)+X_{UO}	Eq. 5		$\tan^{-1}[(7)/(4)]$	(3)+ΔX_D	Eq. 10 + ΔY_D			(11)−(12)	(4) Tan (2)	(13)+(14)	$\tan^{-1}[(13)/(4)]$	(4)/cos(16)	(4)/cos(2)	(17)+(18)	½(19)	(15)/(19)	(11)−(10)t	(22)−(14)	(22)−(13)	(24)/(23)	ΔY_o−(10)avg	(10)avg−(26)avg	Eq. 17 or Fig. 6	(23)(24)/2	$\pi^2[(28)+(29)](20) / (1)^2 (21)$	$1.16e^{-(30)}$
ft.	ft.	ft.	ft.	ft.	degrees	ft.	ft.	ft.	ft.	ft.	ft.	ft.	degrees	ft.	ft.	ft.	ft.		ft.	ft.	ft.		ft.	ft.	ft.	ft.		
-144		-138.1	60.0			-100	60.0	60.0															47.0					
									41.1	18.9		37.1	20.7	53.5		106.7	53.3	0.348			0.5	0.42				0.387	2.60	0.09
	50	-90.3	42.5						40.8	19.2	18.2	37.4	21.0	53.6	53.2	106.8	53.4	0.350	19.4	1.2	0.2	0.17				0.245	1.64	0.23
									40.9	19.1		37.3	20.9	53.5		106.7	53.4	0.350			0.3	0.25				0.300	2.01	0.16
-94		-88.1	41.7			-50	40.6	40.8															28.8					
									30.4	10.4		19.5	22.6	27.1		53.7	26.8	0.363			0.3	0.19				0.346	1.12	0.38
	25								30.6	10.2	9.1	19.3	22.2	27.0	26.6	53.6	26.8	0.360	10.7	1.6	0.5	0.31				0.447	1.46	0.27
									30.5	10.3		19.4	22.4	27.0		53.6	26.8	0.362			0.4	0.25				0.400	1.30	0.32
-69		-63.1	33.2			-25	30.1	30.6															19.7					
									23.3	7.3		12.8	26.0	16.7		32.7	16.3	0.391			0.6	0.25				0.600	1.10	0.39
	15								23.5	7.1	5.5	12.6	25.3	16.6	16.0	32.6	16.3	0.387	7.9	2.4	0.8	0.33				0.693	1.28	0.32
-54		-48.1	26.4			-10	22.7	23.5															14.2					
									21.0	2.5		4.3	26.6	5.6		10.9	5.5	0.394			1.4	0.67				0.857	0.52	0.69
	5										1.8				5.3				3.9	2.1								
-49		-43.1	24.5			-5	19.6	21.0															12.4					
									17.0	4.0		5.8	38.7	6.4		11.7	5.9	0.496			1.7	0.44				1.287	0.67	0.59
	5			2.0	21.8				17.4	3.6	1.8	5.4	35.8	6.2	5.3	11.5	5.7	0.470	5.7	3.9	2.1	0.54				1.431	0.76	0.54
-44 (=ΔX_D)		-38.1	22.5			0	15.3 (10.6 for pores)	17.4															10.6 (=ΔY_o)					
									12.1	5.3		7.1	46.7	7.3		12.6	6.3	0.563			2.3	0.40				1.826	1.12	0.38
	5			2.0	21.8				12.0	5.4	1.8	7.2	47.2	7.4	5.3	12.7	6.3	0.567	7.6	5.8	2.2	0.38		0.50	0.45	1.786	1.09	0.39
-39		-33.1	20.5			+5	9.8	12.0															8.8					
									9.6	2.4		4.2	25.6	5.5		10.8	5.4	0.389			0.7	0.54				0.477	0.87	0.49
	5								9.5	2.5	1.8	4.3	26.6	5.6	5.3	10.9	5.5	0.394	3.1	1.3	0.6	0.46		1.45	0.95	0.442	0.85	0.50
-34		-28.1	18.5			+10	8.9	9.5															7.0					
									5.9	3.6			20.0 (=θ)															
	10										3.6													2.95	1.20			
-24		-18.1	14.2			+20	7.3	5.9															3.3					
									2.3	3.6			20.0															
	10										3.6																	
-14		-8.1	9.4			+30	5.6	2.3															-0.3					
									-0.7	3.0			20.0															
	8.1										3.0																	
-5.9		0.0	3.9			+38.1	4.2	-0.7															-3.3					

Step 3

Equation 27 gives
$S_{min} \cong (4\ Y_{DO}^2/\{\sin[(45^\circ + \theta)/2]\})^{1/2} \cong 3$ m (10 ft)
From Figure 8, at $X_D = 0$, $h_u = Y_U - Y_{\theta U} = 3.6$ m (11.9 ft), and $\theta_u = 21.8^\circ$, Equation 28 gives
$S_{max} \cong (4\ h_u^2/\{\sin[(\theta_u + \theta)/2]\})^{1/2} \cong 12$ m (40 ft)
Use trial drain spacings S = 4.6 m (15 ft), 9.2 m (30 ft), and 13.7 m (45 ft).

Step 4. Phreatic Surface M

See columns 11 and 12 of Figure 8 for the solution for S = 4.6 m (15 ft). Similar analyses were made for S = 9.2 m (30 ft) and S = 13.7 m (45 ft). The resulting phreatic surfaces are plotted in Figure 3.

CONCLUSIONS

1. A method of estimating phreatic surfaces at the midway profile between parallel drains is introduced. Because of the large number of assumptions made in the derivation of practical mathematical analyses, the results must be considered approximate only.
2. The analysis procedure can be based on flow-net analysis or on a completely mathematical analysis. Using the mathematical analysis has the advantage in that it can be computerized by using the procedure from Figure 8 for an infinite-slope seepage source.
3. For a typical problem, the analysis procedure resulted in a range of drain spacings from 4.6 to 13.7 m (15-45 ft), which coincides well with the range commonly used in practice.
4. Further study is needed to define the optimum cross-sectional spacing to use in the analysis of a given drain spacing S. The analysis is sensitive to the cross-sectional spacing used. Using a wider spacing (ΔX in Figure 8) between cross sections results in a greater predicted drawdown. An optimum cross-sectional spacing (ΔX) as a function of drain spacing (S) is expected and needs to be verified by model study and experience.

REFERENCES

1. H. R. Cedergren. Seepage, Drainage, and Flow Nets. Wiley, New York, 1967, pp. 94-98 and 334-344.
2. W. V. Jones and R. Larsen. Investigation and Correction of a Highway Landslide. Proc., 8th Annual Idaho Engineering Geology and Soils Engineering Symposium, Pocatello, 1970, pp. 123-144.
3. T. C. Kenney, M. Pazin, and W. S. Choi. Design of Horizontal Drains for Soil Slopes. Journal of Geotechnical Engineering Division, Proc., ASCE, Vol. 103, No. GT11, Nov. 1977, pp. 1311-1323.
4. R. W. Prellwitz. Analysis of Parallel Drains for Highway Cut-Slope Stabilization. Proc., 16th Annual Idaho Engineering Geology and Soils Engineering Symposium, Boise, 1978, pp. 153-180.
5. A. Casagrande. Seepage Through Dams. In Contributions to Soil Mechanics, 1925-1940, Boston Society of Civil Engineers, 1963, pp. 295-336.
6. M. E. Harr. Groundwater and Seepage. McGraw-Hill, New York, 1962, pp. 52-54 and 64-69.
7. J. N. Luthin. Drainage Engineering. Krieger, Huntington, NY, 1973, pp. 149-169.
8. J. Wesseling. Subsurface Flow into Drains: Vol. 2—Drainage Principles and Applications. International Institute for Land Reclamation and Improvement, Wageninen, Netherlands, 1973, pp. 1-56.

Publication of this paper sponsored by Committee on Subsurface Drainage and Committee on Environmental Factors Except Frost.

Evaluation of Pavement Systems for Moisture-Accelerated Distress

S. H. Carpenter, M. I. Darter, and B. J. Dempsey, Department of Civil Engineering, University of Illinois, Urbana

The occurrence of moisture-accelerated distress (MAD) caused by poor internal drainage in a pavement is predictable after examining components of the pavement and its environment. MAD is defined as any distress primarily caused or accelerated by moisture. A fast, inexpensive method for identifying existing and potential MAD has been developed and provides a valuable tool to the maintenance engineer managing a system of pavements and the design engineer evaluating a single pavement for possible rehabilitation. In the procedure for evaluating MAD the following are done: Extrinsic and intrinsic factors are predicted, the condition of the pavement surface is surveyed, and the pavement is tested. Each of these is considered a level of refinement in determining the occurrence of MAD in the pavement system and represents increased cost. The extrinsic factors in level one are concerned with climatic influences on the moisture state of the pavement. The intrinsic factors are examined for likelihood of internal drainage problems caused by the materials and cross section being used. This provides an index of potential MAD problems. In the condition survey any existing distress on the pavement surface is directly measured. The final step is to conduct physical tests of the pavement, if it is felt that inadequate information has so far been obtained. This testing may be either destructive or nondestructive. By the final evaluation stage, one has sufficient working knowledge to make an accurate judgment as to the existence of or the potential for occurrence of MAD. One or more alternative maintenance and rehabilitation strategies can be selected, based on the evaluation results, to reduce or prevent MAD. The final selection of the alternative is based on the present condition of the pavement, traffic level, economics, and future requirements.

The data presented in this paper are part of an evaluation manual developed for field use by pavement engineers. The manual provides complete descriptions of how to identify pavements with poor internal drainage that potentially could deteriorate prematurely. Four distinct components have been examined that show a relationship to moisture-accelerated distress (MAD): extrinsic factors, intrinsic factors, condition survey, and testing.